Model of the Origin of Rhythmic Population Oscillations in the Hippocampal Slice

ROGER D. TRAUB, RICHARD MILES, ROBERT K. S. WONG

One goal of mammalian neurobiology is to understand the generation of neuronal activity in large networks. Conceptual schemes have been based on either the properties of single cells or of individual synapses. For instance, the intrinsic oscillatory properties of individual thalamic neurons are thought to underlie thalamic spindle rhythms. This issue has been pursued with a computer model of the CA3 region of the hippocampus that is based on known cellular and synaptic properties. Over a wide range of parameters, this model generates a rhythmic activity at a frequency faster than the firing of individual cells. During each rhythmic event, a few cells fire while most other cells receive synchronous synaptic inputs. This activity resembles the hippocampal theta rhythm as well as synchronized synaptic events observed in vitro. The amplitude and frequency of this emergent rhythmic activity depend on intrinsic cellular properties and the connectivity and strength of both excitatory and inhibitory synapses.

RHYTHMICAL OSCILLATIONS IN POPULATION ACTIVITY OCcur in many neuronal systems. They may produce behaviors such as chewing, breathing, and walking. Population oscillations in the cortex are responsible for rhythmical waves in the electroencephalogram (EEG). The functional correlate of cortical rhythms is not known. Wiener (*1*) suggested that the alpha rhythm from visual parts of the cortex subserved a sensory gating function. Hippocampal theta EEG activity can be phase-locked to sniffing in rats (*2*), suggesting that it may be involved in generating rhythmical motor output or in sensory information processing. Repetitive synaptic activation at frequencies in the range of the theta rhythm may also facilitate synaptic plasticity (*3*). Whatever the role of cortical oscillations, the analysis of their generation offers insight into the organization of the neuronal networks involved.

Oscillations in the cortical EEG reflect correlated synaptic inputs in underlying cortical cells. Cellular firing is usually less well correlated with the EEG than are synaptic events (*4, 5*). It is not clear how correlated synaptic inputs can therefore arise. Coherent rhythmic afferent inputs, from the thalamus for instance, may contribute to rhythmicity of the cortical EEG. However, rhythmic synchronous synaptic potentials have also been observed in dual intracellular recordings from hippocampal and cortical slices. In vitro synchronous synaptic events cannot reflect projected activity from another brain region. These cortical regions in isolation can thus autonomously produce population oscillations. Here we discuss a computer model of the CA3 region that reproduces this activity of the hippocampal slice. We then establish some connections between rhythmic oscillations in the slice and EEG waves in vivo, particularly hippocampal theta rhythm.

At least two possible mechanisms might determine the frequency of rhythmical oscillations in a population of neurons: (i) the intrinsic oscillatory properties of the individual cells and (ii) the time courses of synaptic currents. For example, for case (i), in cardiac sinoatrial node cells (*6*), inferior olivary neurons (*7*), thalamocortical relay cells (*8*), and nucleus reticularis thalami (NRT) neurons (*9*), there are intrinsic rhythms determined by the kinetic properties of membrane Ca^{2+} and K^+ currents. When the cells are coupled together via electrotonic junctions (heart and inferior olive) or via inhibitory synapses (NRT), population oscillations emerge at the same, or nearby, frequencies (*10*). For case (ii), on the other hand, Lopes da Silva (*11*) and Freeman (*12*) have demonstrated how the time course of recurrent inhibition can, in effect, filter out a particular population frequency when a network of neurons is driven by appropriate types of noise.

Our model suggests that neither intrinsic cellular properties nor the time course of synaptic currents are sufficient, by themselves, to account for rhythmic population activities in the hippocampal slice. Some of the reasons for this are as follows. (i) Both experimentally and in simulations, the strength (not just the time course) of excitatory and inhibitory synapses influences the amplitude and frequency of population oscillations. (ii) Hippocampal neurons can generate intrinsic bursts, that is, sequences of three or more action potentials; however, population oscillations (detected as synchronized synaptic potentials) can occur at significantly shorter intervals than does bursting in any single neuron. Rhythmic synchronized synaptic potentials may be recorded at intervals as brief as 250 to 300 ms, whereas we have never recorded repetitive bursting in a hippocampal pyramidal cell in vitro at intervals less than 350 ms. Indeed, cell firing is infrequent during rhythmic synchronized activity. (iii) In our model, synchronized synaptic potentials can occur at intervals too long to correspond to any of the synaptic currents. The existence of emergent aspects of the population behavior emphasizes the importance of the computer for this kind of study (*13*).

Our hippocampal model now contains 9900 neurons and can simulate synchronized population bursts that propagate smoothly from one end of a 1-cm longitudinal CA3 hippocampal slice to the other (*14*); a large number of cells is necessary in the model to reproduce the synchronization process that develops locally via recurrent excitatory synapses and at the same time to have sufficiently extended circuitry to allow a propagating wave to occur. Our model contains about half the number of neurons that actually occur in the experimental preparation. Although many of the basic

R. D. Traub is at IBM Research Division, Thomas J. Watson Research Center, Yorktown Heights, NY 10598, and at the Department of Neurology, Columbia University, New York, NY 10032. R. Miles and R. K. S. Wong are in the Department of Neurology, Columbia University, New York, NY 10032.

features previously reported (*13*) are preserved in the large system, new features have emerged. These include complex spatial patterns in the initiation of population discharges and the ability of the system to regulate the spatial coherence of population bursts by changing the mean excitability of the cells.

Synchronized Population Events: Experimental Observations

Synchronized rhythmic cellular activities have been observed in vitro in slices of human lateral temporal neocortex and of monkey and guinea pig hippocampus (*15–18*) as rhythmic extracellular field potentials in apical dendritic layers (*19*) or as repeating simultaneous synaptic potentials in dual intracellular recordings (*15–18*). This behavior does not appear to be an indicator of epileptogenesis.

In vitro synchronized cellular activity can be modified by pharmacologic blockade of fast γ-aminobutyric acid (GABA)–mediated inhibition. In some cases (*15*) such blockade leads to a diminution of synchronized activities. Picrotoxin, a blocker of $GABA_A$ synapses, causes intracellularly recorded simultaneous synaptic potentials to become both larger and less frequent as inhibition is blocked (*18*). The events also become predominantly excitatory as inhibition is blocked (*18*). Schneiderman has observed similar effects on extracellular field potentials as inhibition is progressively blocked with penicillin (*19*). At the stage where fully synchronized epileptiform bursts begin to occur, partially synchronized events may continue to be present (*19*).

A second method for modulating rhythmic activity in the hippocampal slice is to stimulate tetanically an afferent pathway (*20*). Again, synchronized synaptic potentials increase in amplitude and decrease in frequency. The tetanic stimulation affects synaptic transmission along both excitatory and inhibitory pathways. The fact that rhythmic behavior appears after—and its form is modulated by—plastic changes in synaptic function further indicates that this activity is of physiological relevance.

An example of repeating synchronized synaptic potentials in a "normal" (not disinhibited) slice is shown in Fig. 1. This figure illustrates some of the paradoxical features of this type of activity. (i) The shape of synaptic events is not constant and (ii) cellular firing is infrequent. Further evidence for (ii) comes from the small size of the field potentials, less than 0.6 mV, associated with this type of synchronized event (*19*). (iii) An underlying rhythmicity is not always apparent from inspection of a pair of intracellular records, particularly when inhibition is putatively normal; rhythmicity becomes more continuous in intracellular records when inhibition is partly blocked, but even then, the interevent intervals are not precisely constant (*18*, figure 8). The continuous repeating character of the events is apparent in field potential records (*19*) or in plots of total population activity in the model. Our model, based on established physiological principles outlined here, reproduces the basic features of this behavior (Fig. 1B). Activity in the model is driven by random spontaneous bursting of pyramidal cells (*21*). Each partially synchronized event represents an attempt by the neural circuitry to generate a fully synchronized event through the recurrent excitatory synaptic connections. Spread of activity along these connections is limited, however, by cellular refractoriness from previous rhythmic events, and also by synaptic inhibition.

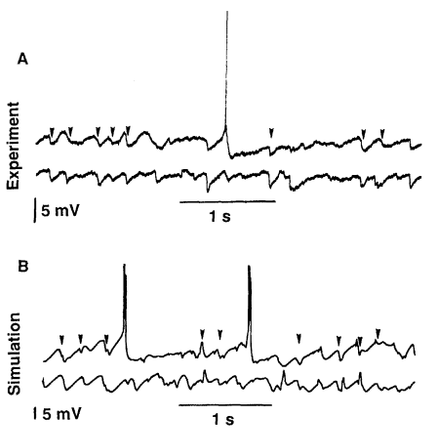

Fig. 1. Synchronized synaptic potentials. (**A**) Simultaneous intracellular potentials from two pyramidal neurons, about 200 μm apart, recorded in stratum pyramidale of the CA3 region of a transverse guinea pig hippocampal slice bathed in normal medium (that is, without blockade of synaptic inhibition). Slice preparation and recording techniques are described in (*28*). The repeating synaptic events, usually inhibitory, are often phase-locked between the two cells. Firing is infrequent. These two cells were not electrotonically coupled. (**B**) Two simultaneous pyramidal cell potentials from a simulation of a network of 9000 model pyramidal cells and 900 inhibitory cells. Portions of these records are clearly rhythmical, whereas in other portions rhythmicity is less clear. Examination of the population as a whole is necessary to see the underlying rhythmicity (Fig. 3). Action potentials are truncated for both experiment and simulation.

Model of the CA3 Region

In the course of our studies of the CA3 region, we have developed a computer model of this structure (*14, 22, 23*). Each neuron in the model is realistically simulated with multiple somatic and dendritic compartments (*24*). The critical features of this model, each justified experimentally, are as follows.

1) Individual CA3 pyramidal neurons generate intrinsic bursts with long, intrinsic afterhyperpolarizations (AHPs) after the burst (*25*). These bursts occur spontaneously, in many neurons, at intervals of between 500 ms to several seconds.

2) The excitatory synaptic connections between pyramidal neurons are powerful enough that a burst in a presynaptic neuron can evoke a burst in a postsynaptic neuron, provided the latter is not refractory from a recent burst or simultaneously inhibited (*18, 26*). Although recurrent excitatory connectivity is limited, there appear to be enough connections so that multiple polysynaptic paths run between any two cells. The network of excitatory synapses is responsible for the synchronization of bursting that occurs when fast inhibition is pharmacologically blocked. A pyramidal cell may respond to an excitatory input with an excitatory postsynaptic potential (EPSP) or with one or two action potentials, if the cell is hyperpolarized or if the presynaptic neuron does not fire a sufficiently prolonged series of action potentials.

3) Excitatory synaptic connections are spatially restricted, at least in a statistical sense (Fig. 2). The evidence for this comes from experiments in longitudinal CA3 slices (*14*). A local shock elicits monosynaptic EPSPs in which the amplitude is smaller in cells situated further from the shock; axon conduction velocity of recurrent excitatory collaterals, determined from experiments such as this, is about 0.5 m/s. On the other hand, a locally synchronized discharge propagates at only 0.1 to 0.2 m/s and requires polysynaptic circuitry. We reproduced these data with a model containing 9000 pyramidal cells in a 40 by 225 array (Fig. 2) with the probability of connection between any pair of cells declining exponentially with distance between the cells.

4) Both fast and slow inhibitory postsynaptic potentials (IPSPs) (*27*) are activated by recurrent local circuitry, with disynaptic fast IPSPs having short latency (a few milliseconds) (*23, 28*). The recurrent circuitry for fast IPSPs has been observed directly, by eliciting disynaptic IPSPs during simultaneous penetrations of pairs of pyramidal cells. The evidence for recurrent activation of slow IPSPs is more indirect. For example, it has been observed that during synchronized bursts occurring in penicillin, CA3 cells develop an AHP that is resistant to intracellular EGTA (*29*), and hence

presumably is not an intrinsic Ca^{2+}-dependent, K^+-mediated potential. During spontaneous "background" behavior (Fig. 1), long-duration hyperpolarizing potentials (presumably slow IPSPs) occur in cells that have not recently fired, making it unlikely that the potentials are intrinsically mediated. Such hyperpolarizing potentials can occur in longitudinal CA3 slices that contain no CA1, hilar, or dentate granule cells that might provide feed-forward excitation onto the cells mediating slow IPSPs. This makes it likely that recurrent circuitry can activate the cells producing slow IPSPs.

The above ideas have been synthesized into a computer model (*14, 30*). This model was developed to analyze evoked activities, lasting 100 or 200 ms, under different conditions of inhibitory blockade. To study spontaneous activity, we endowed at least some of the neurons with the capacity to fire without external (that is, synaptic) stimulation (*31*). We used a random distribution of periodic burst properties and then explored the effects of changing the statistics of the distribution. Spontaneous activities in our model pyramidal cells were determined by assigning to each cell a randomly chosen depolarizing bias current (0.0 to 1.2 nA) and a randomly chosen time constant for relaxation of the intrinsic slow K^+ current. This corresponds to the assumption that if the cells were synaptically isolated, some would burst rhythmically, while others would have various different subthreshold resting potentials. Furthermore, any population rhythmicity that occurs will not simply reflect identical time constants in the various cells for the slow K^+ current. In some simulations our usual distribution of bias currents (as used in Fig. 1) was multiplied by a constant, in effect modifying the excitability of the pyramidal cells (*32*).

Simulation of Rhythmic Population Activities

Although many individual model neurons burst rhythmically when synaptically isolated, the behavior of the system is quite different when the synaptic network is intact. Recurring synaptic potentials are recorded in the various neurons, corresponding to periodicity in the number of cells firing as a function of time (Fig. 1 and Fig. 3, upper trace). The shape of the synaptic potentials is not uniform, as occurs experimentally (Fig. 1). Furthermore, firing of individual cells is both infrequent and not periodic, the latter schematically indicated in the lower section of Fig. 3. The population frequency (that is, the predominant frequency in the upper curve of Fig. 3) is much faster than the frequency at which any of the isolated cells would burst (Fig. 4). All of these cardinal features of the model are robust, in the sense that they persist over a wide choice of values of the system parameters, provided we adhere to the basic structural features of the CA3 region of the hippocampus outlined above. Specifically, population oscillations with these characteristics continue to occur when the following parameters are varied by 50% or more: the strength of excitatory synapses onto pyramidal cells or onto inhibitory cells, the strength of either fast or slow inhibitory synapses, and the conductance of the slow Ca^{2+}-dependent K^+ current.

To compare the model better with experiment and to understand the mechanism by which a model based on such simple principles generates complex behavior, we tested the effects of varying basic parameters. We varied parameters alone and in combination, although not all possibilities could be tried, a typical simulation taking up to 8 hours of computation time. We were especially interested in the determinants of the amplitude and frequency of the rhythmic oscillation, as well as the pattern of initiation and time course of the individual synchronized events.

Fast inhibition. Let us consider first "fast" $GABA_A$-dependent inhibition since this can be blocked pharmacologically. As has been discussed elsewhere (*13, 19*), progressive blockade of fast inhibition leads to an increase in amplitude of synchronized excitatory synaptic potentials, with a decrease in frequency. Eventually, synchronized population bursts occur with interburst intervals of several seconds; in the presence of penicillin, population bursts may be preceded by one or more partially synchronized bursts (*13, 19*). In the model, decreasing fast inhibition also increases the amplitude of partially synchronized events and diminishes their frequency, but the frequency does not diminish to the same extent in simulations (down to about 1.5 Hz) as it does in experiments (down to about 0.5 Hz). The behavior in the model when fast inhibition is completely blocked depends on the strength of the excitatory synapses and on the mean excitability of the pyramidal cells. If excitatory synaptic strength is only just powerful enough to permit burst propagation between resting neurons, then fully synchronized population discharges do not occur in simulations; even with fast inhibition totally blocked, only partially synchronized discharges occur. When excitatory synaptic strength is larger, for example, 2 to 2.5 times threshold for burst propagation, then fully synchronized population discharges do occur, with regularly repeating pattern. The number of interspersed partially synchronized events depends then on cellular excitability; partially synchronized events interspersed with fully synchronized events occur only with larger cellular excitabilities. Unlike the experimental case, we do not see periods between population bursts as long as 5 s or more, unless artificial situations are created, such as allowing no spontaneous bursting except in one neuron forced to burst at the desired intervals. It is possible that experimentally, under conditions of full $GABA_A$ blockade and population bursting, a particularly slow form of inhibition is expressed, a form of inhibition not included in our model.

Recurrent excitation. When fast inhibition is present (for example, with a peak unitary IPSP conductance of 10 nS), then progressively

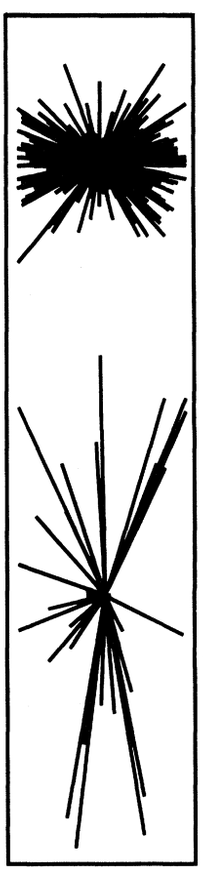

Fig. 2. Structure of the model. The 9000 pyramidal cells lie in a 40 by 225 array. A 4 by 225 array of inhibitory cells lies superimposed. The output connections of a single inhibitory cell (**above**) and a pyramidal cell (**below**) are shown, illustrating the different spatial distributions and axonal divergences. Each pyramidal cell has an average of 22 outputs. Each inhibitory cell has an average of 220 outputs (*30*).

increasing the strength of excitatory synapses (beyond an initial value above threshold for burst propagation) also has the effect of progressively increasing the amplitude of partially synchronized events and diminishing their frequency. When excitatory synapses are powerful enough (more than three times threshold for burst propagation), short trains of two to four synchronized bursts in a row are seen, at intervals of 100 to 200 ms. These bursts are reminiscent of polyspikes in EEG records; they have not been observed in slices, to our knowledge. On the other hand, when excitatory synapses between pyramidal cells are removed (but pyramidal cells still excite inhibitory cells as before), then the population activity becomes "disorganized," that is, no rhythmic oscillations are apparent. Thus, recurrent excitation is indeed critical for rhythmicity in this system; it is not the case here that recurrent inhibition alone leads to rhythmicity by, in effect, filtering noisy background activity.

Cellular excitability: Effects on amplitude and frequency of rhythm. Reducing the mean excitability from that in Figs. 1 and 3 (wherein 1300 cells are capable of spontaneous bursting) significantly increased the interval between partially synchronized events. Intervals of more than 500 ms could be observed when only 36 cells were spontaneously active. Such large intervals between events are longer than the duration of slow IPSPs in the model (the time constant for decay of the slow IPSP conductance in the model being 100 ms); thus, slow inhibition is not the only determinant of frequency of synchronized events, at least under certain conditions.

Diminishing excitability has two different effects: it reduces the number of spontaneously bursting cells and lengthens their interburst intervals; but it also tends to make propagation of bursting from cell to cell more difficult, as if excitatory synapses had become less effective. To allow for this second effect, we examined excitability changes at two different levels of excitatory synaptic strength ("weak" and "strong," with the unitary conductance in the strong case twice that of the weak case, and the weak case still above threshold for burst propagation between resting neurons). In either case, reducing excitability of the pyramidal cells led to a diminished frequency of partially synchronized events. With strong excitatory synapses, mean excitability had little effect on the amplitude of partially synchronized events. With weaker excitatory synapses, increasing excitability diminished the amplitude of the events (except at extremely weak excitabilities, that is, with only three cells capable of spontaneous activity). Schwartzkroin and Haglund (*15*) increased the excitability of their slices by raising extracellular K^+ concentration, and they observed an increase in frequency and decrease in amplitude of synchronized synaptic potentials, consistent with the behavior of our model with weaker excitatory synapses. However, extracellular K^+ increases will also affect transmitter release, as well as altering in a depolarizing direction the reversal potential of Cl^- IPSPs (*33*).

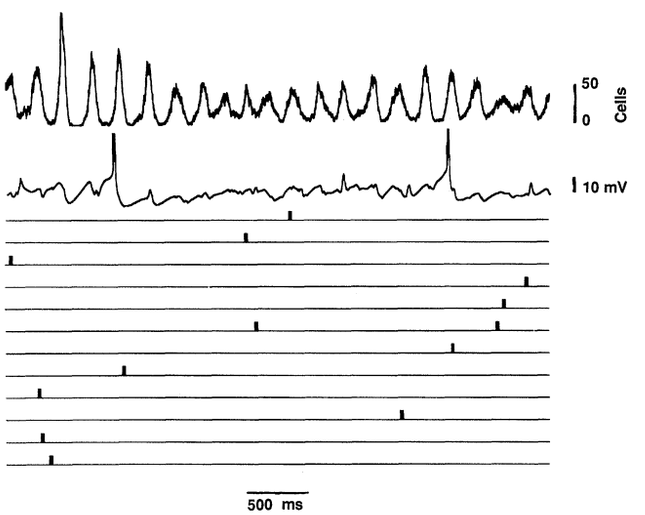

Fig. 3. Rhythmic population activity with nonrhythmical bursting in individual cells. The simulation is the same as in Fig. 1B. (**Upper trace**) The number of pyramidal cells (9000 in all) that are depolarized more than 20 mV (the potential at which they are capable in the model of generating axonal output). (**Middle trace**) Potential of a single cell. It bursts at a much slower rate than the population oscillatory rate. (Action potentials are truncated.) The cell demonstrates repeating synaptic potentials in which the shape changes with the relative admixture of excitatory, fast inhibitory, or slow inhibitory inputs. (With different parameters, for example, larger excitatory strength and lower cellular excitability, synaptic potentials are predominantly excitatory.) (**Lower section**) For 12 different neurons a vertical bar is inscribed at times when the respective neuron fires a burst. The resulting "musical score" emphasizes the irregular firing patterns of the individual cells, in contrast to the global oscillation of the population as a whole. When the cells are synaptically isolated from each other, any cell bursting repeatedly will burst rhythmically (not shown).

Cellular excitability: Effects on pattern of initiation. An example of a sudden reduction in excitability of the pyramidal cells is shown in Fig. 5. Not only does the frequency of population events suddenly decrease, but the pattern of initiation changes as well. When excitability is high, partially synchronized events are initiated by the approximately simultaneous (to within 108 ms) spontaneous bursts of dozens of neurons (31 in Fig. 5). Bursts in the other participating cells develop by excitatory synaptic spread of activity along complex chains [an example in a small model is shown in (*13*, figure 7)]. The spread of activity is one-to-one or one-to-many at the beginning of the event (Fig. 5). Subsequent pyramidal cell firing recruits inhibitory neurons, so that neurons drawn into later parts of the event are usually hyperpolarized and are recruited only when two or more of their excitatory synaptic precursors have already been recruited, that is, spread of activity becomes many-to-one. When too few cells are firing to sustain this many-to-one propagation, the event terminates. In contrast, at lower excitabilities (Fig. 5B, right), partially synchronized events are initiated by a smaller number of spontaneously bursting neurons, only one in the case illustrated. The mechanisms of subsequent synaptic spread of activity are then similar to the high excitability case, although sometimes (as in Fig. 5) one can visualize the spatial propagation of activity. This latter effect is a result of the (statistical) spatial restriction of the excitatory connections.

In Fig. 5, excitatory spread occurs to only one, two, or three of any given cell's connected followers, even though every pyramidal cell contacts, on average, 20 other pyramidal cells. The reason is that the interval between partially synchronized bursts (hundreds of milliseconds) is shorter than the time it takes for a bursting neuron to recover enough so that bursting can be induced in it by a burst in a single synaptic precursor; this latter interval is usually 1 s or more. Thus, many of a cell's followers will be refractory from having fired during recent partially synchronized events. The long duration of the intrinsic AHP of hippocampal neurons appears critical for this aspect of population behavior. Other cells will be rendered refractory by rapid recruitment of recurrent inhibition. The regulation by synaptic inhibition of propagation along excitatory pathways has been demonstrated experimentally (*18*) and also studied in simulations (*13, 23*). To know exactly which cells will be recruited into a given event, one needs to know not only the initiating cells but also the recent past of the entire system (to determine the refractoriness of the various cells) and the full network structure of the system. In the examples we have studied, there is no apparent repeating subgroup of firing cells, despite the periodic activity of the population as a whole. It remains to be determined whether the exact cellular composition of firing neurons during the different partially synchronized events carries biologically meaningful information.

Simulations, as in Fig. 5, show that approximately synchronized synaptic potentials can occur even between neurons several millimeters apart; that is, low-amplitude population oscillations are coherent over distances that are long compared with the distribution of the synaptic connections. Schwartzkroin and Haglund (*15*) have observed this phenomenon of long-range synchrony in slices of monkey hippocampus with electrode separations of more than 3 mm, and we have observed it in partially disinhibited guinea pig slices. Furthermore, at least when the cells are not too excitable, there should be, on average, phase lags between synaptic potentials in cells sufficiently separated; this too has been observed by Schwartzkroin and Haglund (*15*). Our model predicts that such phase lags will diminish as cellular excitability increases, owing to the simultaneous initiation of synchronized events over a broad region (as in Fig. 5B, left).

What is the physical basis for the spatial coherence of bursting, given that excitatory synaptic connections tend to be localized? If the simulation of Fig. 1 is repeated, but with the array divided by a cut into two pieces (40 by 112 pyramidal cells and 40 by 113 pyramidal cells), each piece generates rhythmical partially synchronized events at the same mean frequency as the whole array; activities in the two pieces, however, move in and out of phase with each other. This confirms what is intuitively clear, that it is local synaptic connections that keep different regions of the model "locked together." Pieces as small as 40 by 28 cells will oscillate at about the same frequency as the full array, although the oscillations become irregular in such small pieces; thus, the frequency of oscillation is apparently determined by the properties of (more-or-less) localized neuronal ensembles. When a midline cut permits excitatory connections, but not inhibitory connections, to cross, then the entire neuronal ensemble still oscillates in phase. In our model, inhibition is not critical for coupling together population oscillations in neighboring neuronal ensembles.

Slow inhibition. Blocking slow inhibition in the model had profound effects on rhythmic activity. When cellular excitability is sufficiently high and slow IPSPs are blocked, partially synchronized events do not occur, and continuous irregular activity takes place in the population; individual cells fire in bursts at irregular intervals. When cellular excitability is low, on the other hand, with slow IPSPs blocked, the population activity resembles EEG delta waves; large waves of activity lasting about 1 s each, of changing morphology, occur and repeat with intervals of 2 to 3 s. Now that a specific blocker of $GABA_B$ synapses is available (*34*), these model predictions should be experimentally testable.

Comparison with Hippocampal Theta Rhythm

Hippocampal theta, or rhythmical slow activity, is an EEG rhythm recorded in rodents, rabbits, and some other species (*5*). It has two pharmacologically distinct forms, one observed during certain waking behaviors (such as locomotion), the other observed during immobility or urethane anesthesia. Typical theta frequencies are 4 to 8 Hz. The medial septal nucleus–diagonal band of Broca is critical for generation of theta, and the septal nucleus contains autonomous oscillatory properties (*35*) that, in principle, could synaptically induce oscillations at the same frequency in hippocampus and entorhinal cortex (in a manner similar to the way the sinoatrial node of the heart normally drives rhythms in the rest of the heart). Alternatively, it may be that acetylcholine release from septal neurons is permissive for network oscillations depending otherwise only on hippocampal or entorhinal circuitry. There is some evidence for the latter possibility, in that hippocampal slices can generate a theta-like rhythm when a cholinergic agent is perfused (*36*). In addition, injection into the hippocampus of muscarinic agents can elicit theta rhythm in vivo (*37*). We therefore consider it useful to ask if the rhythmic population activity in the slice in our model shares any features with in vivo theta rhythm. Our model is not intended to represent theta generation in vivo in all its aspects.

Cyclic excitability. A series of simulations was done in which 600 cells were excited by injection of currents timed at different phases of the underlying population rhythm. The "evoked response," that is, the number of cells firing immediately after the current injection, varied with the relative timing of the stimulus and the underlying rhythm. As a population event begins, many cells receive subthreshold EPSPs, which, on average, will tend to increase the size of an evoked response. As the event continues, inhibition is recruited, so that, on average, cells are relatively hyperpolarized, decreasing the

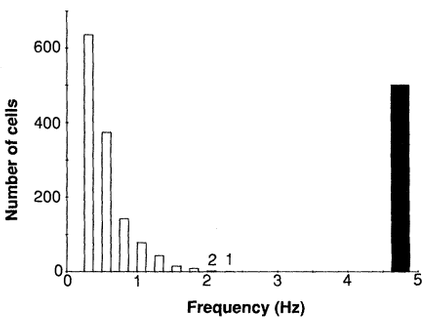

Fig. 4. The frequency of population rhythmicity is much faster than the frequency of any individual cell in isolation. The open bars are a histogram of the bursting rates of the pyramidal cells in isolation with the excitability parameters as in Figs. 1 and 3, but with no synaptic interactions. The bin size is 0.25 Hz. The solid bar is the frequency of the population oscillation (that is, the mean frequency of the oscillation in the top trace of Fig. 3) when synapses are functional. The population frequency for this simulation (4.75 Hz) is related to the time course of slow IPSPs in the model (the time constant for relaxation of the slow IPSP current is 100 ms).

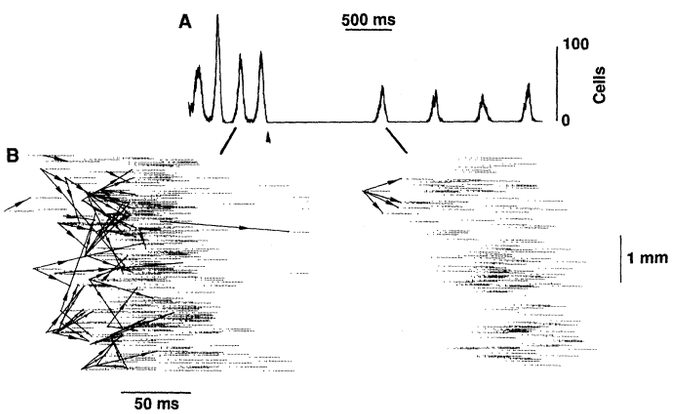

Fig. 5. Effect of cellular excitability on frequency and structure of simulated rhythmical activity. (**A**) Number of cells depolarized beyond 20 mV (above resting potential) as a function of time. Mean cellular excitability begins at a high level, but at the time marked by the arrowhead it is abruptly dropped (4.8-fold). Both frequency and amplitude then decrease. (The amplitude decreases in part because the lower excitability makes it more difficult for bursting to propagate from one cell to another.) (**B**) The structure of individual population waves at two levels of excitability, on an expanded time scale. The horizontal streaks represent bursts in individual cells at various spatial locations. The solid lines with arrows indicate synaptic connections from cells that burst spontaneously ("initiating cells") to those of their followers, which also burst during the event. When excitability is high (left), there are 31 different initiating cells scattered across the array. Other cells are induced to fire by spread of activity along synaptic connections, but (because of cell refractoriness and inhibition) propagation occurs across only certain connections. When excitability is low (right), there are fewer initiating cells. In the example shown, there is only one initiating cell. Arrows are drawn in only for the first generation of synaptic spread of activity.

size of an evoked response. Similar cyclic variations in evoked response amplitude have been observed in vivo during theta rhythm (*38*, 39). This phenomenon has been modeled at the single cell level by Leung (*40*).

Phase resetting. When a stimulus to the model is delivered before a partially synchronized burst is due to occur, and if the stimulus is large enough to evoke a partially synchronized burst, then the phase of subsequent events is reset (*41*). This phenomenon, too, has been observed in vivo (*39, 42*) and in slices (*15*).

Spatial coherence. Population discharges occur approximately synchronously along the entire length of the model, provided cellular excitability is high enough (Fig. 5). It is this spatial synchrony of firing that leads to the spatial synchrony of synaptic potentials confirmed experimentally in vitro (*15, 16*). It has also been observed that in vivo theta activity can be coherent over distances of several millimeters along the length of the hippocampus (*43*).

Correlation between cellular firing and population waves. During a typical population wave, such as illustrated in Fig. 3, about 250 pyramidal cells burst, that is, about 2.8% of the total population. But there are 450 inhibitory cells in the model with a firing pattern consisting of rapid trains of action potentials, that is, firing in the pattern of typical interneurons; these are the cells that, in the model, produce slow inhibition. About 280 interneurons, or 62% of the respective population, fire during the same population event. Schwartzkroin and Haglund (*15*) observed that cells with "interneuron-like" firing characteristics were much more likely (even more likely than in our model) to fire during a partially synchronized event than were cells with pyramidal cell–like firing characteristics. In vivo, it has also been noted that repetitively firing neurons are more likely to fire during a theta wave than are putative pyramidal cells (*5*).

Hippocampal sharp waves. By properly regulating certain model parameters, particularly the strength of the fast inhibitory synapses, it is possible to have the model generate synchronized bursts of any amplitude. Graded synchronized bursts, producing sharp waves in the local EEG, are observed in the hippocampus of normal rats (that is, rats without seizures) during consummatory behaviors such as drinking (*44*). The model suggests that increasing pyramidal cell excitability alone will not, by itself, account for this EEG phenomenon, since sharp waves can have rather long periods between them (seconds). Increasing the excitability of all of the pyramidal cells in the model tends to decrease the interval between partially synchronized events. Our model is consistent with the idea that sharp waves could occur under conditions of low excitability and partial blockade of inhibition, as suggested by others (*44*).

Conclusion

We have discussed here an emergent population oscillation in a model of the hippocampal CA3 region. The model is based on established principles concerning the physiology of single cells and the properties and spatial distribution of unitary synaptic actions. The model is consistent with numerous experiments on the response of the slice to brief shocks. Its emergent oscillatory behavior also is consistent with experimental evidence. We have suggested that the model may therefore be useful in understanding some puzzling features of EEG rhythms. A significant aspect of these results is that we have demonstrated that it is possible to describe a piece of mammalian cortex in some detail.

Our model makes specific predictions: (i) recurring synchronized synaptic potentials should be sensitive to total blockade of slow IPSPs; (ii) the intervals between these potentials should be little affected when the slice is bisected, provided recordings are both taken from the same half; (iii) phase lags between synaptic potentials in cells widely separated should diminish when cellular excitability is increased; and (iv) recurring synchronized synaptic potentials should be sensitive to blockade of recurrent excitatory synapses.

REFERENCES AND NOTES

1. N. Wiener, *Cybernetics* (MIT, Cambridge, 1961).
2. B. R. Komisaruk, *J. Compar. Physiol. Psychol.* **70**, 482 (1970); K. Semba and B. R. Komisaruk, *Electroencephalogr. Clin. Neurophysiol.* **44**, 61 (1978).
3. J. Larson and G. Lynch, *Science* **232**, 985 (1986).
4. O. Creutzfeldt, in *Handbook of Electroencephalography and Clinical Neurophysiology*, O. Creutzfeldt, Ed. (Elsevier, Amsterdam, 1974), vol. 2c, pp. 5–55.
5. G. Buzsáki, L.-W. S. Leung, C. H. Vanderwolf, *Brain Res.* **287**, 139 (1983).
6. D. C. Michaels, E. P. Matyas, J. Jalife, *Circ. Res.* **58**, 706 (1986); **61**, 704 (1987).
7. R. Llinás and Y. Yarom, *J. Physiol. (London)* **315**, 549 (1981); *ibid.*, p. 569; *ibid.* **376**, 163 (1986); M. Deschênes, M. Paradis, J. P. Roy, M. Steriade, *J. Neurophysiol.* **51**, 1196 (1984); J. P. Roy, M. Clerq, M. Steriade, M. Deschênes, *ibid.*, p. 1220.
8. H. Jahnsen and R. Llinás, *J. Physiol. (London)* **349**, 205 (1984); *ibid.*, p. 227.
9. C. Mulle, A. Madariaga, M. Deschênes, *J. Neurosci.* **6**, 2134 (1986).
10. In the case of NRT, it may be required that the time course of the inhibitory synaptic currents be "matched" to the kinetics of removal of inactivation of the low-threshold Ca^{2+} current.
11. F. H. Lopes da Silva *et al.*, *Prog. Brain Res.* **45**, 281 (1976).
12. W. J. Freeman, *Biol. Cybern.* **35**, 21 (1979).
13. R. D. Traub, R. Miles, R. K. S. Wong, L. S. Schulman, J. H. Schneiderman, *J. Neurophysiol.* **58**, 752 (1987).
14. R. Miles, R. D. Traub, R. K. S. Wong, *ibid.* **60**, 1481 (1988).
15. P. A. Schwartzkroin and M. M. Haglund, *Epilepsia* **27**, 523 (1986).
16. R. Miles and R. K. S. Wong, unpublished data.
17. P. A. Schwartzkroin and W. D. Knowles, *Science* **223**, 709 (1984).
18. R. Miles and R. K. S. Wong, *J. Physiol. (London)* **388**, 611 (1987).
19. J. H. Schneiderman, *Brain Res.* **398**, 231 (1986).
20. R. Miles and R. K. S. Wong, *Nature* **329**, 724 (1987).
21. There are two mechanisms for generation of rhythmic events that we consider unlikely: a small set of "pacemaker" pyramidal neurons that bursts during each synchronized event, and driving of the rhythm solely by inhibitory neurons. We have never observed pyramidal neurons that spontaneously burst with periods as short as 250 ms, even after recording from many thousands of cells. Spontaneous bursts tend to occur with intervals of 500 ms and above; intervals as short as 350 ms have been observed on occasion [R. K. S. Wong and D. A. Prince, *J. Neurophysiol.* **45**, 86 (1981)]. It is therefore unlikely that there exists a small set of pacemaker pyramidal cells driving the rhythm. Conceivably, a set of inhibitory neurons might somehow be synchronized with each other and oscillate at this period, perhaps analogous to population oscillations in NRT, but inhibitory neurons are not known to possess currents with the requisite time course, and this mechanism would not explain the EPSPs that are often intermixed in the complex synaptic potentials.
22. R. D. Traub and R. K. S. Wong, *Science* **216**, 745 (1982).
23. R. D. Traub, R. Miles, R. K. S. Wong, *J. Neurophysiol.* **58**, 739 (1987).
24. R. D. Traub, *Neuroscience* **7**, 1233 (1982).
25. R. K. S. Wong and D. A. Prince, *J. Neurophysiol.* **45**, 86 (1981).
26. R. Miles and R. K. S. Wong, *J. Physiol. (London)* **373**, 397 (1986).
27. By "fast" inhibition, we mean Cl^--dependent inhibitory potentials mediated by $GABA_A$ receptors. The time constant for decay of the underlying conductance is 20 ms or less. We distinguish this from "slow" inhibition, mediated presumably by $GABA_B$ receptors activating K^+ currents. Slow IPSPs can last for several hundred milliseconds.
28. R. Miles and R. K. S. Wong, *J. Physiol. (London)* **356**, 97 (1984).
29. P. A. Schwartzkroin and C. E. Stafstrom, *Science* **210**, 1125 (1980).
30. In addition to the 9000 pyramidal cells in the model, there are 900 inhibitory cells, 450 producing fast and 450 producing slow IPSPs. Each neuron has, on average, 20 excitatory and 20 inhibitory inputs. The probability for an excitatory connection from a cell is proportional to $e^{-x/30}$, where x is the intercellular distance in cell diameters along the long axis of the array. For an inhibitory connection, the probability is proportional to $e^{-x/6}$. We estimated the spatial distribution of the excitatory synapses from physiological measurements and simulations (*14*). Anatomical studies suggest that the axons of inhibitory cells in the hippocampus are spatially more restricted than are the axons of pyramidal cells [D. M. Finch, N. L. Nowlin, T. L. Babb, *Brain Res.* **271**, 201 (1983); N. Tamamaki, K. Watanabe, Y. Nojyo, *ibid.* **307**, 336 (1984); L. Seress and C. E. Ribak, *J. Neurocytol.* **14**, 717 (1985); P. Somogyi, M. G. Nunzi, A. Gorio, A. D. Smith, *Brain Res.* **259**, 137 (1983)]. Single pyramidal cells were simulated as in (*24*), except that dendrites contained only passive membrane, in order to reduce computation time. The time constants (β_q^{-1}) for relaxation of an intrinsic current (a Ca^{2+}-dependent K^+ current) in the different cells were distributed from 500 to 2500 ms. Bias currents ranged from 0 to 1.2 nA. An example of the distribution of the resulting spontaneous burst frequencies is shown in Fig. 4. Neurons eliciting convulsant-resistant inhibition (slow IPSPs) were simulated by omitting Ca^{2+}-dependent currents. Reversal potentials for EPSPs, fast IPSPs, and slow IPSPs were +60, −15, and −25 mV, respectively, relative to resting potential. EPSPs onto bursting neurons developed in the dendrites; their conductance had a time course proportional to $te^{-t/3}$ (t in milliseconds), with a peak conductance of 15 nS (in the dendrites). With such a conductance, cell-to-cell transmission of bursting could occur in the absence of refractoriness and simultaneous inhibition. Peak conductances of up to 45 nS were investigated. EPSPs onto inhibitory cells developed on

the soma. The conductance time course was proportional to te^{-t}, with a peak of 120 nS. These properties allowed a single presynaptic action potential to evoke an action potential in an inhibitory neuron. Fast IPSPs developed on the soma and adjacent compartments, with conductance time course rising linearly over 2 ms and then decaying with a time constant of 7 ms; the peak value was different in different simulations. The peak value was usually 10 nS, but values from 0 to 15 nS have been investigated. Slow IPSPs developed in the dendrites; they grew steadily over 40 ms and decayed with a time constant of 100 ms. The time course of the simulated slow IPSP after a local shock is shown in (*14*, figure 1). The output of pyramidal neurons was distributed to follower cells after a delay proportional to cell separation along the long axis of the array; this delay corresponded to axon conduction delays. An axon conduction velocity of 0.5 m/s was used. Details are in (*14*). Programs were written in Fortran, optimized for the IBM 3090 vector compiler. A simulation of 3 s of neural activity consumed about 6.6 hours of computation time on the 3090 computer.

31. There is little precise experimental guidance on how to do this. The necessary experiment would involve synaptically isolating all the neurons in a population from each other without changing any of their intrinsic properties and then characterizing the spontaneous activities of a large sample of the cells.
32. There is another type of synchronized activity that occurs in hippocampal slices wherein all forms of chemical synaptic actions have been blocked. This activity consists of repeating, large-amplitude population spikes [C. P. Taylor and F. E. Dudek, *Science* **218**, 810 (1982); J. G. R. Jefferys and H. L. Haas, *Nature* **300**, 448 (1982)], probably synchronized by electric field interactions [C. P. Taylor and F. E. Dudek, *J. Neurophysiol.* **52**, 126 (1984); R. D. Traub, F. E. Dudek, C. P. Taylor, W. D. Knowles, *Neuroscience* **14**, 1033 (1985)]. We shall not treat this type of activity in this article because during partially synchronized bursts of the type we are considering, the extracellular potentials in the cell body layer are too small to be detected with present recording methods.
33. S. J. Korn *et al.*, *J. Neurophysiol.* **57**, 325 (1987).
34. P. Dutar and R. A. Nicoll, *Nature* **332**, 156 (1988).
35. O. S. Vinogradova, E. S. Brazhnik, A. M. Karanov, S. D. Zhadina, *Brain Res.* **187**, 353 (1980).
36. J. Konopacki, M. B. MacIver, B. H. Bland, S. H. Roth, *ibid.* **405**, 196 (1987). It has been suggested, however, that carbachol may simply alter the intrinsic properties of hippocampal neurons [L.-W. S. Leung and C. Y. Yim, *Neurosci. Res. Commun.* **2**, 159 (1988)].
37. R. Malisch and T. Ott, *Neurosci. Lett.* **28**, 113 (1982).
38. A. P. Rudell, S. E. Fox, J. B. Ranck, *Exp. Neurol.* **68**, 87 (1980).
39. G. Buzsáki, E. Grastyán, J. Czopf, L. Kellényi, O. Prohaska, *Brain Res.* **225**, 234 (1981).
40. L.-W. S. Leung, *J. Neurophysiol.* **52**, 1051 (1984).
41. R. D. Traub, R. Miles, R. K. S. Wong, *IEEE Eng. Med. Biol. Mag.* **7**, 31 (1988).
42. G. Buzsáki, E. Grastyán, I. N. Tveritskaya, J. Czopf, *Electroenceph. Clin. Neurophysiol.* **47**, 67 (1979).
43. G. Buzsáki and F. H. Gage, in *Memory Mechanisms: A Tribute to G. V. Goddard*, M. Corballis, K. White, W. Abraham, Eds. (Erlbaum, Hillsdale, NJ, in press).
44. G. Buzsáki, *Brain Res.* **398**, 242 (1986); S. S. Suzuki and G. K. Smith, *Electroenceph. Clin. Neurophysiol.* **67**, 348 (1987).
45. Supported by IBM, The Klingenstein Foundation, and NIH. We thank G. Buzsáki and L. S. Schulman for helpful discussions and A. Rossi for invaluable assistance in optimizing Fortran code.

Research Articles

Hydrogen Tunneling in Enzyme Reactions

YUAN CHA,* CHRISTOPHER J. MURRAY,† JUDITH P. KLINMAN‡

Primary and secondary protium-to-tritium (H/T) and deuterium-to-tritium (D/T) kinetic isotope effects for the catalytic oxidation of benzyl alcohol to benzaldehyde by yeast alcohol dehydrogenase (YADH) at 25 degrees Celsius have been determined. Previous studies showed that this reaction is nearly or fully rate limited by the hydrogen-transfer step. Semiclassical mass considerations that do not include tunneling effects would predict that $k_H/k_T = (k_D/k_T)^{3.26}$, where k_H, k_D, and k_T are the rate constants for the reaction of protium, deuterium, and tritium derivatives, respectively. Significant deviations from this relation have now been observed for both primary and especially secondary effects, such that experimental H/T ratios are much greater than those calculated from the above expression. These deviations also hold in the temperature range from 0 to 40 degrees Celsius. Such deviations were previously predicted to result from a reaction coordinate containing a significant contribution from hydrogen tunneling.

ELECTRON TUNNELING IN PROTEINS HAS BEEN EXTENSIVELY studied (*1*). Rapid, long-distance electron transfer between donor and acceptor sites appears well established (*2*). Although quantum-mechanical tunneling of particles heavier than the electron has been actively studied in solid-state, gas-phase, and solution reactions (*3*), nuclear tunneling in proteins has received relatively little attention. In this article we present evidence that nuclear tunneling contributes to enzymatic reaction rates under biologically relevant conditions. The phenomenon of hydrogen tunneling is an especially promising area to pursue, in that hydrogen has a small mass and the kinetics of protium can be compared with its isotopes, deuterium and tritium (*4*). Detection of H-tunneling in chemical reactions has relied heavily on either the detection of anomalously large isotope effects or the comparison of Arrhenius plots for H transfer to that for either D or T. Given the enhanced probability for H tunneling, greater curvature is anticipated in its Arrhenius plot. A manifestation of this property is a decrease in the magnitude of the intercept obtained on extrapolation to infinite temperature such that the Arrhenius prefactors are ordered as $A_H < A_D < A_T$ (*3*).

The detection of nuclear tunneling in enzymatic reactions presents several experimental challenges. In enzymatic systems, diffusional binding processes, rather than chemical transformations, may limit catalysis (*5, 6*). Even in the event that an elementary chemical step can be isolated at a single temperature, alterations in temperature can lead to changes in rate limitation, giving rise to artifactual curvature in Arrhenius plots. In 1985 Saunders (*7*) demonstrated that the relation of D/T to H/T kinetic isotope effects can show significant deviations from semiclassical limits when tunneling contributes to the H-transfer step. We have experimentally verified

The authors are at the Department of Chemistry, University of California, Berkeley, CA 94720. The order of the first two authors is arbitrary.

*Present address: Department of Chemistry, Rockefeller University, New York, NY 10021.
†Present address: Department of Chemistry and Biochemistry, University of Arkansas, Fayetteville, AR 72701.
‡To whom correspondence should be sent.